

Figure S1. Cell line authentication, related to Figure 1 and 2. The authenticity of the genomic-engineered KRAS-G12V isogenic cell lines and patient-derived colorectal cancer cell lines was experimentally verified by western blotting of the cell lysates using KRAS-G12V or pan-KRAS antibody.

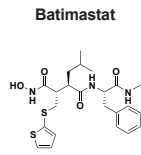
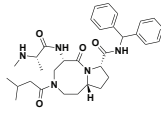
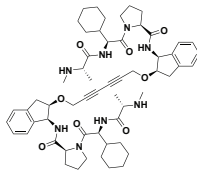
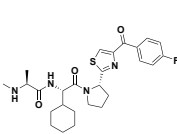
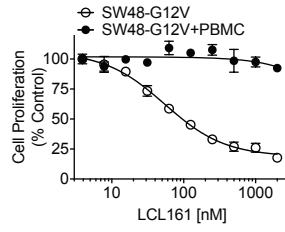
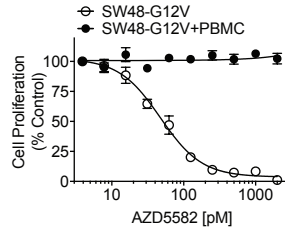
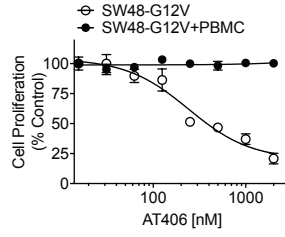
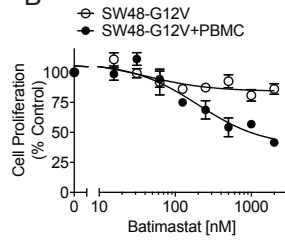
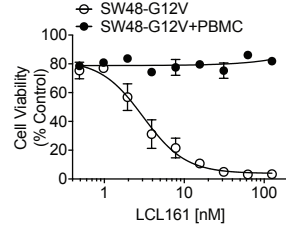
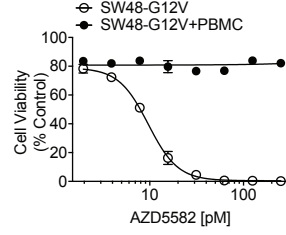
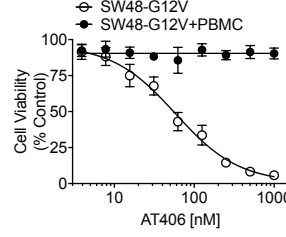
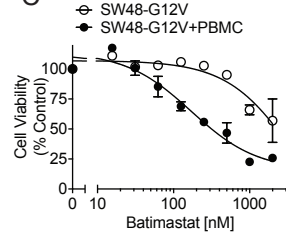
A**AT406****AZD5582****LCL161****B****C**

Figure S2. Assay and screening performance evaluation, related to Figure 1 and 2.

(A-B) S/B and Z' calculated at PBMC/cancer cell ratio of 5 from **(A)** image- and **(B)** biochemical-based readouts. The data are presented as mean \pm SD from 4 replicate wells.

(C-F) S/B and Z' calculated from six independent assay plates in the presence **(C and D)** or the absence **(E and F)** of PBMC using the image-based cell proliferation readouts **(C and E)** or the biochemical-based cell viability readouts **(D and F)**. The data are presented as mean \pm SD from 16 replicate wells. For dots that show no error bar, the error bar was smaller than the dot.

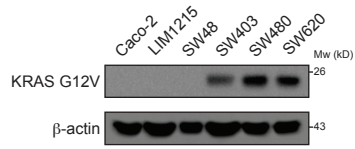
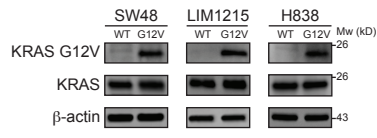


Figure S3. Dose-response curves of batimastat and three additional IAP antagonists in HTiP assay, related to Figure 2. (A) Chemical structure of the compounds as indicated. **(B-C)** The corresponding dose-dependent inhibition curves of SW48-G12V cell growth from **(B)** image-based cell proliferation and **(C)** biochemical-based cell viability readouts. The data are presented as mean \pm SEM from four replicate wells.